MEET3-3
Invited

Alternative methods to suppress surface recombination for GaN-based micro-light emitting diodes

Sheng Hang[1,2], Chunshuang Chu[1,2], Le Chang[1,2], Hua Shao[1,2], Yonghui Zhang[1,2], Quan Zheng[3], Qing Li[3,*], Zi-Hui Zhang[1,2,*]

zh.zhang@hebut.edu.cn, dxjtxmb@126.com

[1]State Key Laboratory of Reliability and Intelligence of Electrical Equipment, Hebei University of Technology, 5340 Xiping Road, Beichen District, Tianjin, 300401, China

[2]Key Laboratory of Electronic Materials and Devices of Tianjin, School of Electronics and Information Engineering, Hebei University of Technology, 5340 Xiping Road, Beichen District, Tianjin, 300401, China

[3]State Key Engineering Center of Flat-Panel-Display Glass and Equipment, 369 Zhujiang Road, High-tech Zone, Shijiazhuang, Hebei Province 050035, People's Republic of China

Keywords: GaN-based µLED, EQEs, SRH recombination, sidewall defects

ABSTRACT

The surface recombination caused by sidewall defects is a key obstacle for GaN-based micro-light-emitting diodes. In this report, we summarize different methods for suppressing the surface recombination that have been proposed by our group.

1 Introduction

Thanks to various superiorities over conventional LCD and OLED display, e.g., high resolution, low power consumption, high brightness, flexibility, fast response and high reliability [1, 2], GaN-based micro-light emitting diodes(µLED)-based display have gained a growing interest in many optical applications such as smart watches, mobile phones, TVs, laptops, micro-projection displays, augmented reality and virtual reality [3-5]. Although the development prospects of µLED-based display are promising, there are still quite a few obstacles that need to be addressed, such as the mass transfer and full-color conversion technology [6, 7]. In addition to these two technical issues in the fabrication of µLED display array, another key problem is the quite low EQE (external quantum efficiency) when the µLED chip size is smaller than 50 × 50 µm^2. This is mainly attributed to the surface nonradiative recombination caused by the sidewall defects, which is negligible for large-size device [8, 9]. It well known that such low EQE for µLED cannot guarantee the luminance requirements of display. Therefore, it is necessary to take measures to alleviate the impact of surface defects on the µLED performance. During the past decades, tremendous efforts have been made. Firstly, Tian et al. have attempted to take the thermal annealing process to reduce the defect density[9]. However, the plasma-caused damages cannot be completely removed by the thermal annealing process. Hence, additional measures have been proposed, such as the sidewall passivation by using the plasma-enhanced chemical vapor deposition (PECVD) or atomic layer deposition (ALD) systems [10, 11]. The results show that such sidewall passivation is helpful to reduce the sidewall imperfections. Furthermore, the sidewall chemical treatment is combined with the sidewall passivation to further eliminate the surface defects [12]. It indicates that there is a homogenized light emission across the mesa of µLED after taking the chemical treatment and sidewall passivation, which proves the strong suppression for sidewall defects [13]. However, the sidewall defects cannot be completely resolved only by means of the above methods taken during the fabrication process. Therefore, more techniques should be taken to suppress sidewall defects. It is well known that µLEDs have better current spreading effect when compared with large size LED device [14], which means that the current can easily reach the defected sidewall regions. Here we propose alternative methods to suppress the sidewall SRH nonradiative recombination by tunning the lateral current spreading, which keep the injection current apart from the mesa edge. Such confinement also facilitates hole injection into the active region. In this work, two µLED designs have been demonstrated and fabricated. The results indicate the surface recombination is effectively suppressed and hole injection is also enhanced for this two µLED designs. As a result, the improved optical power and EQE can be obtained.

2. Results and discussion

In this work, aiming at tunning the current spreading and suppressing surface nonradiative recombination. Two novel µLED designs have been proposed, which can be summarized as followed: (a) thinning the quantum barriers to manage the current spreading length [15] and (b) adopting the step-type quantum wells with slightly varied InN composition that is essentially important for yellow µLEDs [16].

2.1 Properly thinning the quantum barriers to manage the current spreading

In order to manage the lateral current spreading effect. Firstly, we attempt to properly reduce the vertical resistivity of µLED by decreasing the quantum barrier thickness so that current can easily inject into the active region rather than spreading to the mesa edges. Thus, only few carriers are consumed by sidewall defects. In this work, three types of μLEDs with different quantum barrier thicknesses are investigated. The quantum barrier thickness for μLED I, II, and III are 6 nm, 9 nm and 12 nm, respectively. All the investigated GaN-based blue μLEDs have the chip dimension of 10 × 10 μm^2. The calculated results in Fig.1 indicate that the EQE and the optical power both get enhanced when the quantum barrier thickness decreases, e.g., LED I. The experimentally measured EQEs for μLEDs I and III are shown in inset Fig. 1(a), which also shows the same trend as the numerical calculation results.

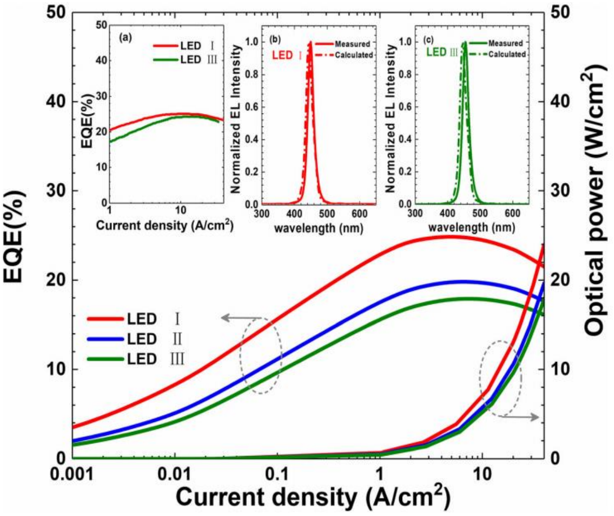

Fig.1 Calculated EQE and optical power density in terms of the injection current density for μLEDs I, II, and III, respectively. Inset Fig.1(a) shows the experimentally measured EQE for μLEDs I and III, respectively. Inset figures Figs.1 (b) and 1(c) present the measured and numerically calculated EL spectra for μLEDs I, and III. Data for inset Figs (b) and (c) are obtained at the current density of 40 A/cm^2.

The numerically calculated SRH and radiative recombination rate are presented in the insets for Figs.2 (a)-(c) for different device. It indicates that the surface nonradiative recombination becomes extremely strong at mesa edges and even higher than the radiative recombination. We then show the ratios between the SRH recombination and the radiative recombination at the edge for the mesa. The results indicate that the ratio for R_{SRH}/R_{rad} at the mesa edge increases as the quantum barrier get thicker, which is attributed to the significantly increased surface nonradiative recombination rate. As we have proposed, thick quantum barriers promote the current spread to mesa edges and further lead to the surface nonradiative recombination. Therefore, properly thinning the quantum barriers for μLED is very helpful to manage the current spreading and suppress sidewall SRH nonradiative recombination.

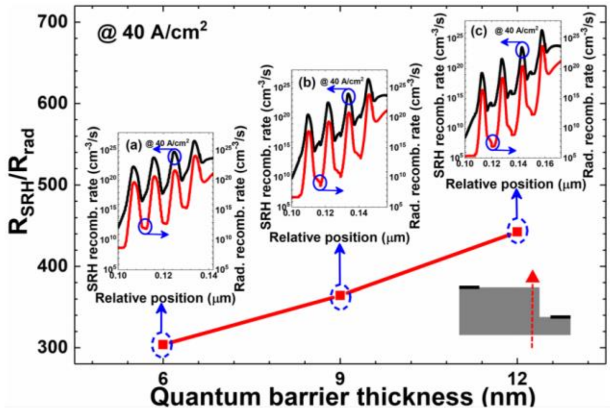

Fig. 2 Ratios of the integrated SRH recombination (SRH) rate and the integrated radiative recombination rate for μLEDs I, II, and III. Inset figures (a), (b), and (c) are the profiles for SRH recombination (SRH) rate and the radiative recombination rate at the mesa edge for μLEDs I, II, and III, respectively. Data are calculated at the current density of 40 A/cm^2.

2.2 Adopting step-type quantum wells to tune the current distribution

Next, targeting at improving the EQEs of yellow μLEDs with high InN compositions, we find that it is still necessary to suppress the sidewall SRH nonradiative recombination for yellow μLEDs. Therefore, another method to engineer the current spreading effect has been proposed, such that by replacing traditional quantum wells of 3-nm-thick $In_{0.30}Ga_{0.70}N$ by step-type quantum wells of $In_{0.25}Ga_{0.75}N$ (1.5 nm)-$In_{0.35}Ga_{0.65}N$ (1.5 nm). The schematic diagram for investigated devices is shown in the Fig. 3(a). By doing that, a reduced valence band barrier height for holes can be obtained, which facilitate hole injection into the active region. Then, a suppressed SRH nonradiative recombination can be also obtained, which is due to the fact that the holes prefer to be vertically injected into the active region instead of spreading to the mesa edge. Meanwhile, the polarization mismatch between the quantum wells and barriers can be decreased, which increases the overlap for electron and hole wave functions. More importantly, we selectively calculate the EL intensity for Device 2-1, 2-2 and 2-3 with the step-type quantum wells of $In_{0.20}Ga_{0.80}N$-$In_{0.35}Ga_{0.65}N$, $In_{0.15}Ga_{0.85}N$-$In_{0.35}Ga_{0.65}N$ and $In_{0.10}Ga_{0.90}N$- $In_{0.35}Ga_{0.65}N$, respectively. Our results show in Fig.1(b) that there is a significantly blue shift of the wavelength for Devices 2-1, 2-2 and 2-3, and this is not observed for Device 2. This indicates that Device 2 with such InN slightly varied step-type quantum well possesses an increased overlap level of electron and hole wave functions without affecting the emission wavelength.

Table.1 Information of device size and device structure for Devices R1, 1, R2, 2, R3, 3, R4 and 4.

Device	Device size	Device structure
R1	$5 \times 5\ \mu m^2$	w/o step-type quantum wells
1		with step-type quantum wells
R2	$10 \times 10\ \mu m^2$	w/o step-type quantum wells
2		with step-type quantum wells
R3	$15 \times 15\ \mu m^2$	w/o step-type quantum wells
3		with step-type quantum wells
R4	$50 \times 50\ \mu m^2$	w/o step-type quantum wells
4		with step-type quantum wells

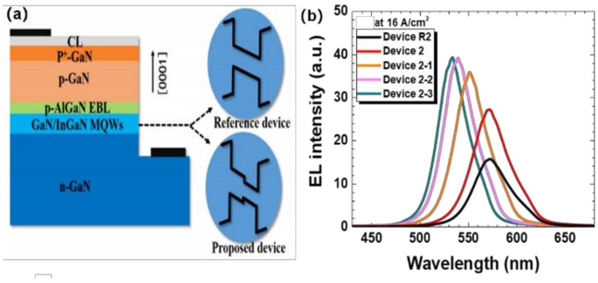

Fig. 3. (a) Schematic diagram for the investigated reference device and the proposed device with step-type quantum wells. CL: current spreading layer, (b) EL intensity for Device R2, 2, 2-1, 2-2, 2-3. Data are selected at the current intensity of 16 A/cm^2.

Then, the EQEs in term of the injection current density are calculated shown in the Fig. 4 (a). It can be found from Fig. 4(a) that the EQEs for Devices 1, 2, 3 and 4 with step-type quantum wells have been enhanced when compared with their counterparts. Furthermore, Fig. 4 (b) also indicates the optical power as the function of injection current density for different device. All the Devices 1, 2, 3 and 4 have the enhanced optical power when compared with Devices R1, R2, R3 and R4, which is consistent with the EQEs profiles shown in Fig. 4 (a). These results prove that adopting the step-type quantum wells is very helpful to improve the performance of μLEDs. This is due to the fact that the μLEDs with step-type quantum wells possess an enhanced carrier injection, which leads to the increased radiative recombination in the active region. Besides, such improved hole injection efficiency also makes carriers less spread to the mesa edge, which further decrease the SRH nonradiative recombination caused by the sidewall defects.

To further reveal the internal device physics when the step-type quantum wells are applied, we selectively show the hole concentration and SRH recombination rate in the last quantum well closest to the p-EBL for Devices R2 and 2 in Figs. 5(a), (b) and (c). As shown in Fig. 5(a), the horizontal hole concentration for Device 2 is greatly improved when compared to Device R2, which is the signature of enhanced hole injection efficiency for Device 2 with the step-type quantum wells. Moreover, the normalized hole concentration profile indicates that for Device 2 with the step-type quantum wells, the injection holes spread less to the mesa edge, which is attributed to the reduced valence band barrier height in the MQWs for Device 2. Furthermore, we present the SRH

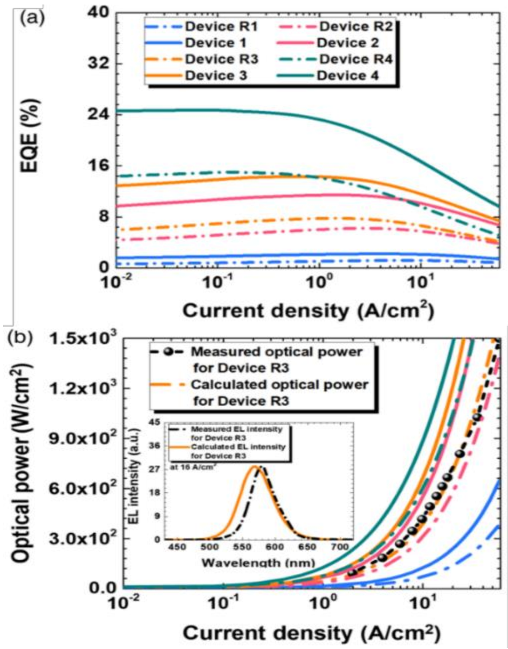

Fig. 4. Numerically calculated (a) EQE and (b) optical output power for Devices R1 and 1, R2 and 2, R3 and 3, R4 and 4. Inset in (b) shows the experimentally measured and numerically calculated electroluminescent intensity for Device R3 at the injection current level of 16 A/cm^2. The measured optical power for Device R3 is also presented in (b).

recombination rate in the active region at the mesa edge in Fig. 5 (c). The results here indicate that Device 2 with the step-type quantum well possess the increased SRH recombination rate when compared with their counterparts. As is known, the SRH recombination rate is proportional to carrier concentration. Thanks to the better hole injection capability for Device 2, both the SRH recombination and radiative recombination can be increased for Device 2 with the step-type quantum wells.

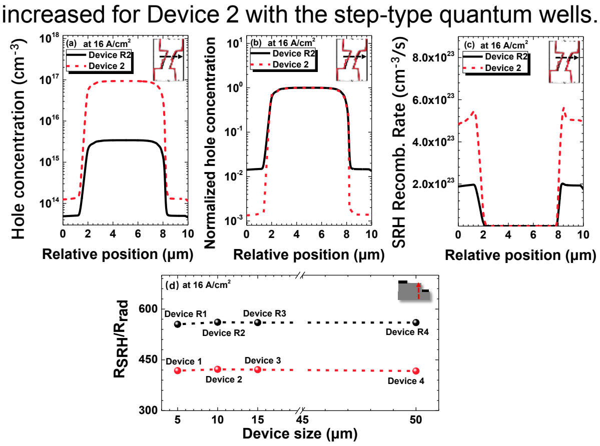

Fig. 5. (a) Horizontal hole distribution profiles and (b) normalized horizontal hole distribution profiles in the eighth quantum well for Devices R2 and 2. (c) Horizontal SRH recombination rate in the eighth quantum well for Devices R2 and 2. (d) Ratios

between the integrated SRH radiative recombination rate in the active region at mesa edge for Devices R1, 1, R2, 2, R3, 3, R4 and 4. The data are calculated at the injection current level of 16 A/cm^2.

Furthermore, we also present the ratios between the integrated SRH recombination rate and integrated radiative recombination rate (R_{SRH}/R_{rad}) in the active region at the mesa edge for Devices R1 and 1, R2 and 2, R3 and 3, R4 and 4 in Fig. 5 (d). It indicates that the values of R_{SRH}/R_{rad} are significantly reduced for Devices 1, 2, 3, and 4 when we compare with Devices R1, R2, R3, and R4, respectively. Therefore, the results here further emphasize that the step-type quantum wells can significantly improve the hole injection efficiency and effectively suppress the consumption of holes by surface nonradiative recombination for GaN-based yellow µLEDs.

3 Conclusion

In this work, novel physics understanding for GaN-based µLEDs has been proposed, such that the SRH nonradiative recombination can be suppressed by managing the current spreading effects to make less injection current reach the mesa edge. Accordingly, two proposed µLED device designs based on this the theory are demonstrated. Thanks to the suppressed SRH recombination caused by sidewall defects, the proposed devices both exhibit enhanced performance if compared with the reference device.

References

[1] H. X. Jiang and J. Y. Lin, Nitride micro-LEDs and beyond--a decade progress review, Opt Express, 21 Suppl 3, A475-484 (2013).

[2] T. Wu, C.-W. Sher, Y. Lin, C.-F. Lee, S. Liang, Y. Lu, S.-W. Huang Chen, W. Guo, H.-C. Kuo and Z. Chen, Mini-LED and Micro-LED: Promising Candidates for the Next Generation Display Technology, Applied Sciences, 8 (9) (2018).

[3] N. Li, K. Han, W. Spratt, S. Bedell, J. Ott, M. Hopstaken, F. Libsch, Q. Li and D. Sadana, Ultra-low-power sub-photon-voltage high-efficiency light-emitting diodes, Nature Photonics, 13 (9), 588-592 (2019).

[4] G. Tan, Y. Huang, M. C. Li, S. L. Lee and S. T. Wu, High dynamic range liquid crystal displays with a mini-LED backlight, Opt Express, 26 (13), 16572-16584 (2018).

[5] K. Zhang, D. Peng, K. M. Lau and Z. Liu, Fully-integrated active matrix programmable UV and blue micro-LED display system-on-panel (SoP), Journal of the Society for Information Display, 25 (4), 240-248 (2017).

[6] L. Zhang, F. Ou, W. C. Chong, Y. Chen and Q. Li, Wafer-scale monolithic hybrid integration of Si-based IC and III-V epi-layers-A mass manufacturable approach for active matrix micro-LED micro-displays, Journal of the Society for Information Display, 26 (3), 137-145 (2018).

[7] H. M. Kim, M. Ryu, J. H. J. Cha, H. S. Kim, T. Jeong and J. Jang, Ten micrometer pixel, quantum dots color conversion layer for high resolution and full color active matrix micro‐LED display, Journal of the Society for Information Display, 27 (6), 347-353 (2019).

[8] F. Olivier, S. Tirano, L. Dupré, B. Aventurier, C. Largeron and F. Templier, Influence of size-reduction on the performances of GaN-based micro-LEDs for display application, Journal of Luminescence, 191, 112-116 (2017).

[9] P. Tian, J. J. D. McKendry, Z. Gong, B. Guilhabert, I. M. Watson, E. Gu, Z. Chen, G. Zhang and M. D. Dawson, Size-dependent efficiency and efficiency droop of blue InGaN micro-light emitting diodes, Applied Physics Letters, 101 (23) (2012).

[10] R. T. Ley, J. M. Smith, M. S. Wong, T. Margalith, S. Nakamura, S. P. DenBaars and M. J. Gordon, Revealing the importance of light extraction efficiency in InGaN/GaN microLEDs via chemical treatment and dielectric passivation, Applied Physics Letters, 116 (25) (2020).

[11] C.-M. Yang, D.-S. Kim, S.-G. Lee, J.-H. Lee, Y. S. Lee and J.-H. Lee, Improvement in Electrical and Optical Performances of GaN-Based LED With SiO2/Al2O3 Double Dielectric Stack Layer, IEEE Electron Device Letters, 33 (4), 564-566 (2012).

[12] W. H. Choi, G. You, M. Abraham, S.-Y. Yu, J. Liu, L. Wang, J. Xu and S. E. Mohney, Sidewall passivation for InGaN/GaN nanopillar light emitting diodes, Journal of Applied Physics, 116 (1) (2014).

[13] M. S. Wong, D. Hwang, A. I. Alhassan, C. Lee, R. Ley, S. Nakamura and S. P. DenBaars, High efficiency of III-nitride micro-light-emitting diodes by sidewall passivation using atomic layer deposition, Opt Express, 26 (16), 21324-21331 (2018).

[14] J. Kou, C.-C. Shen, H. Shao, J. Che, X. Hou, C. Chu, K. Tian, Y. Zhang, Z.-H. Zhang and H.-C. Kuo, Impact of the surface recombination on InGaN/GaN-based blue micro-light emitting diodes, Optics Express, 27 (12), A643-A653 (2019).

[15] L. Chang, Y.-W. Yeh, S. Hang, K. Tian, J. Kou, W. Bi, Y. Zhang, Z.-H. Zhang, Z. Liu and H.-C. Kuo, Alternative Strategy to Reduce Surface Recombination for InGaN/GaN Micro-light-Emitting Diodes—Thinning the Quantum Barriers to Manage the Current Spreading, Nanoscale Research Letters, 15 (1) (2020).

[16] H. Shao, C. Chu, C. M. Chuang, S. Hang, J. Che, J. Kou, K. Tian, Y. Zhang, Q. Zheng, Z. H. Zhang, Q. Li and H. C. Kuo, Step-type quantum wells with slightly varied InN composition for GaN-based yellow micro light-emitting diodes, Appl Opt, 60 (11), 3006-3012 (2021).